Chapter 2
Theory of Supercooled Liquids and Glasses

In this chapter I will attempt to describe the phenomenological understanding of supercooling and the glass transition. A glass is generally defined [25, 44] as an amorphous solid that has experienced a glass transition. This obviously raises the question of what constitutes a glass transition, which is a subject that requires significantly more discourse.

2.1 Kinetics of the Glass Transition

In order to correctly understand the changes which occur during the glass transition, we must first establish certain properties in both the equilibrium liquid and metastable supercooled liquid.

In the equilibrium liquid (above the melting point T_m) structural rearrangements occur due to diffusion, D, which, in the case of a low Reynolds number fluid with spherical particles, is related to the viscosity, η, by the Stokes-Einstein equation:

$$D = \frac{k_B T}{6\pi \eta R} \tag{2.1}$$

where k_B is Bolztmann's constant, T is the temperature, and R is the particle radius. In most cases [44] the viscosity is well described by the Arrhenius equation:

$$\eta(T) = \eta_0 \exp\left(\frac{E}{k_B T}\right) \tag{2.2}$$

where η_0 is a material dependent constant, and E is an activation energy. Along with the average structural relaxation time, many other relaxation times, such as dielectric relaxation, also have an Arrhenius temperature dependence. For clarity, a relaxation time is defined as the time taken for a system to return to equilibrium after a perturbation. At temperatures above the melting point the time dependence

T. Farmer, *Structural Studies of Liquids and Glasses Using Aerodynamic Levitation*, Springer Theses, DOI: 10.1007/978-3-319-06575-5_2,

of relaxation processes is a simple Debye exponential, which is equivalent to $\beta = 1$ in the Kohlrausch-Williams-Watts (KWW) [73] equation:

$$\phi(t) = \exp\left(-(t/\tau)^{\beta}\right) \tag{2.3}$$

where τ a characteristic relaxation time, and $\varphi(t)$ is the relaxation function [15], which is related to the measured quantity $\sigma(t)$ by:

$$\phi(t) = [\sigma(t) - \sigma(\infty)]/[\sigma(0) - \sigma(\infty)]. \tag{2.4}$$

It can be shown that due to the unique properties of exponential behaviour, the relaxation has no dependence on the previous behaviour of the system; the relaxation time is determined only by the temperature the system is at, not by previous temperatures [32].

By contrast, once the liquid is in the metastable supercooled state the relaxation becomes non-exponential [5], and is often well described by the complete KWW Eq. (2.3) with $0 < \beta < 1$. The value of β depends not only upon the material in question but also on the specific relaxation process. Along with the change in time dependent behaviour, the temperature dependence of the average relaxation time can also deviate strongly from the Arrhenius behaviour shown above. This deviation is also seen in the viscosity, and is often well described, albeit over only a few orders of magnitude [5], by the Vogel-Tammann-Fulcher (VTF) [21, 64, 70] equation:

$$\eta(T) = \eta_0 \exp\left(\frac{E}{k_B(T - T_0)}\right) \tag{2.5}$$

where T_0 is the temperature at which the viscosity (or relaxation) is predicted to become infinite. The extent to which the viscosity deviates from Arrhenius behaviour can vary quite significantly, as shown in Fig. 2.1. This leads to a classification of glass forming liquids depending on the extent to which their viscosity becomes non-Arrhenius in the supercooled region; strong liquids, where SiO_2 is the archetype, show little deviation from Arrhenius behaviour, whereas fragile liquids, such as o-terphenyl (OTP) show a marked deviation and are better described by the VTF equation. However, despite the improved description of fragile liquids by the VTF equation relative to Arrhenius behaviour, it is still only sufficient over a few decades of viscosity [5]. Hodge [32] determined that there is a correlation between the fragility of a glass-forming liquid and the extent to which its relaxation function is non-exponential.

From this it can be seen that as the temperature of a supercooled liquid is being reduced, the time it takes for structural relaxations to occur increases very rapidly. If the cooling rate is kept constant, then at a certain temperature there will no longer be sufficient time for the liquid to return to equilibrium before the temperature is reduced. At this temperature the liquid undergoes a kinetic transition to the glassy phase and the structure is effectively fixed on an experimental timescale. This is often defined [25, 44] as ~100 s, which corresponds to a viscosity of $\sim 10^{12}$Pa s. It is also apparent from this definition of the glass transition that it is dependent on the rate at which the liquid is cooled; a slower cooling rate will

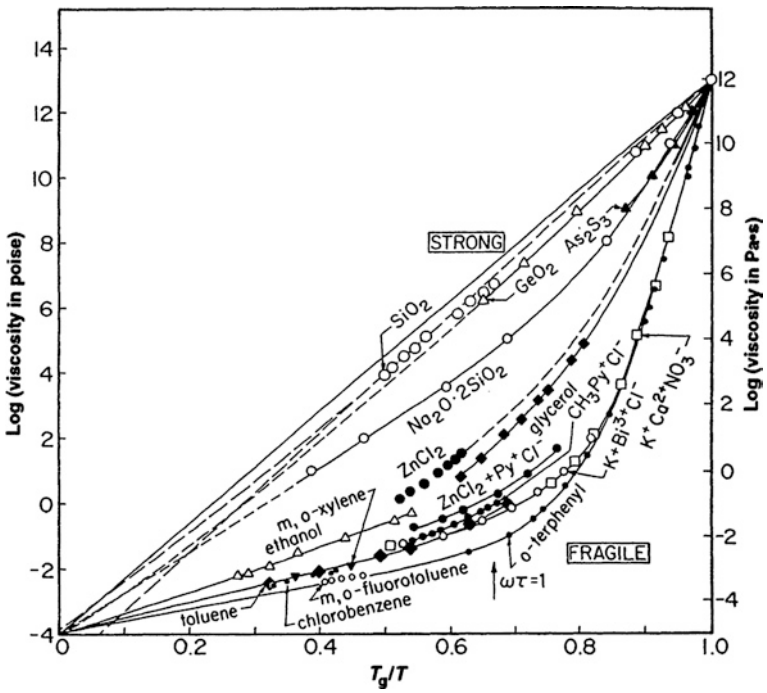

Fig. 2.1 A graph showing the wide range of viscosity behaviours of glass forming liquids as the temperature, T, approaches the glass transition temperature, T_g. (Reproduced in part from Angell [4], reprinted with permission from AAAS. Originally from Angell [3], © 1991, with permission from Elsevier.)

allow the liquid to retain its metastable equilibrium to a lower temperature than a faster cooling rate. Therefore the glass transition temperature is actually a range, determined by the cooling rate. However because of the rapid increase in viscosity with a reduction in temperature, the glass transition temperature is only weakly dependent on the cooling rate; Ediger et al. [18] suggest a temperature difference of 3–5 K with an order of magnitude change in the cooling rate. From both of these points it is apparent that the glass transition temperature is actually an arbitrary temperature range based on both the quench rate and the time over which we measure structural relaxations. The latter of these points is highlighted in Fig. 2.2 which shows the temperature dependence of the frequency dependent specific heat capacity in glycerol [8].

The change to super-Arrhenius relaxations in the supercooled regime only affects some relaxation processes, generally termed α relaxations [62]. In fragile glasses other relaxation processes (β processes) have been observed to retain their Arrhenius nature, and so at a certain temperature there is a splitting of relaxation processes [15]. This can be seen in the case of dielectric relaxation in Fig. 2.3. The specific mechanism behind this splitting and the resulting β relaxations is not well established [22, 56].

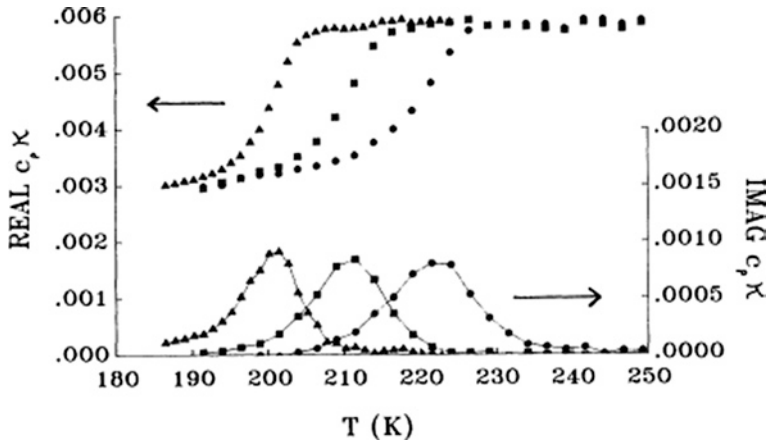

Fig. 2.2 The real and imaginary product of the frequency dependent specific heat capacity and the thermal conductivity for glycerol, as determined by Birge and Nagel [8], © 1985 by the American Physical Society. The three different frequencies are 0.62 Hz (*triangles*), 34 Hz (*squares*), and 1,100 Hz (*circles*). The glass transition temperature for glycerol, as determined by differential scanning calorimetry, is 180 K. A sharp decrease in specific heat capacity is indicative of a glass transition, as discussed in Sect. 2.2

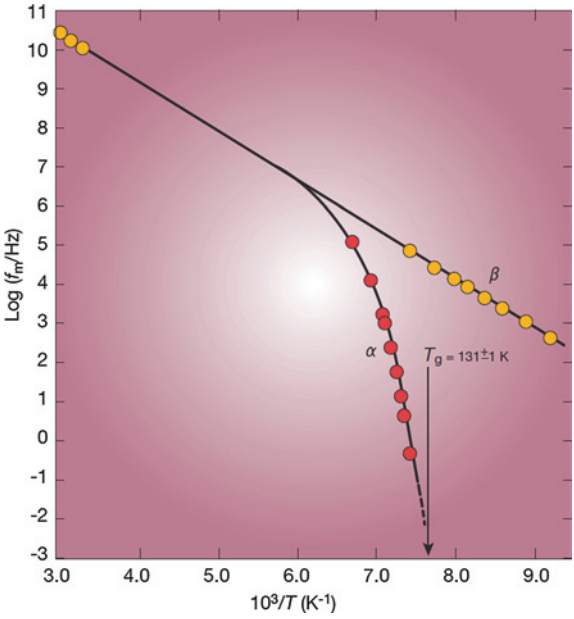

Fig. 2.3 The splitting of the peak dielectric relaxation frequency of a chlorobenzene/cis-decalin mixture into two separate relaxations. Figure reproduced from Debenedetti and Stillinger [15], Reprinted by permission from Macmillan Publishers Ltd: © 2001)

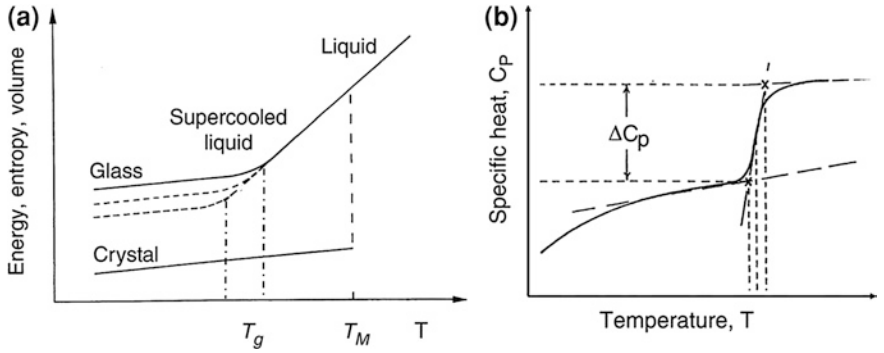

Fig. 2.4 A schematic showing the change in (**a**) the first and (**b**) the second derivatives of the free energy at the glass transition. The *dash-dotted lines* in (**a**) highlight that T_g occurs over a range of temperatures dependent on the quench rate. It is important to note that while the specific heat capacity in (**b**) changes sharply, it is not discontinuous (Adapted from Greaves and Sen [25], Reprinted with permission from Taylor and Francis Ltd. http://www.informaworld.com)

2.2 Thermodynamics of the Glass Transition

While so far I have only discussed the kinetics of the glass transition, it is important to also consider the thermodynamics. At the glass transition temperature range there is a significant change in the thermodynamic properties. This is clearly seen in both the first and second derivatives of the free energy, such as the entropy and the specific heat capacity, as shown schematically in Fig. 2.4. Despite the fact that over the range there is a large change in the specific heat capacity, it is observable that there is no discontinuity [4]. This eliminates the possibility that the glass transition is either a first order or second order phase transition as understood by the Ehrenfest classification [19]. Although Fig. 2.4 does not show a discontinuity in the entropy indicative of a first order phase transition, it does highlight an interesting paradox that was first established by Kauzmann [37]. As the specific heat capacity of the liquid is higher than that of the solid states, its entropy decreases more rapidly with decreasing temperature. Therefore if the metastable liquid state can be maintained without either crystallization or glass formation intervening, there will be a temperature, T_K, at which the entropy of the liquid decreases below that of the corresponding crystal. Although this is not forbidden in itself, it creates the possibility that the entropy could drop to zero at $T > 0$ K, thus violating the third law of thermodynamics. There are a few possible resolutions to Kauzmman's paradox, one of which involves the formation of an 'ideal glass', which would of course have a solid-like heat capacity, at T_K. This concept hints at the possibility of a true thermodynamic phase transition, and it has been suggested [4] that the kinetic glass transition that is experimentally observed could be masking this. In the case of fragile liquids, where there is often a large change in the specific heat capacity upon crystallization, T_K is often not very far below T_g. Despite this it has not been experimentally possible to access T_K without the intervention of either vitrification or crystallization.

2.3 Theoretical Descriptions of the Viscous Slowdown

For completeness some mention should be made of a few of the theoretical descriptions of the increase in relaxation times as the glass transition is approached.

The approach of Cohen and Turnbull [12, 68] was to state the necessary condition for a molecular rearrangement to occur in terms of a 'free volume'. The origin of this was related to the observation of a marked decrease in fluidity (or increase in viscosity) with applied pressure. By considering the diffusion as requiring motion into a free volume of critical size (assuming no hop back occurs), they reduced the problem of the glass transition to the determination of the temperature dependent free volume distribution. In this description the glass transition occurs when the energy required to redistribute the free volume becomes large.

Adam and Gibbs [2] chose instead to describe a configuration in terms of the fraction of cooperatively rearranging regions; these are regions of a specific size within which a configurational rearrangement can take place effectively independently of the macroscopic system. Consideration of the temperature dependent transition probability allows the determination of a minimum critical size of these regions, below which the transition probability is zero. As this critical size increases with decreasing temperature, there exists a temperature at which it diverges, which equates to the glass transition. It is important to note that both the free volume theory [12] and the configuration entropy theory [2] have derived equivalent equations to the VTF equation.

The final approach that will be discussed is that of mode coupling theory (MCT) [7, 23, 40]. It was pointed out [7] that in the liquid state the time dependent density correlation function tends to zero, as after a sufficiently long time diffusion has caused the density at any point to be independent of that after time t. However in the glassy state if we assume there is no diffusion then the density correlations do not decay. The key concept of MCT is an attempt to describe the approach to this glassy state by means of a non-linear density correlation function; this acts in such a way that the density correlation function has a memory. This non-linearity couples the size of the density fluctuations with their ability (through the longitudinal viscosity) to decay; therefore as the density fluctuations increase, the viscosity increases, which in turn reduces the decay of the density fluctuations. It is important to note that the original versions of MCT [7] resulted in a divergence which was not observed; this has since been corrected by modifications (see [15]).

2.4 Avoided Crystallization

It is also instructive to consider glass formation from the perspective of avoided crystallization. In order for a crystal structure to form, either heterogeneous or homogeneous nucleation must occur. Heterogeneous nucleation takes place at sites that are preferential to nucleation, such as seed crystals or solid surfaces. By contrast,

homogenous nucleation is the formation of crystalline nuclei purely from statistical atomic rearrangements. Below a certain volume these nuclei are unstable and will tend back to the general liquid structure. However once a certain critical volume is achieved it becomes energetically favourable for crystal to grow [69]. This occurs when the decrease in free energy due to increasing the crystal volume overcomes the increase in free energy required to form the crystal-liquid interface, which is dependent on the surface area as opposed to the volume. Due to the temperature dependence of the free energy difference required for nucleation, the critical size reduces as the liquid is more deeply supercooled. However a competing factor occurs in the form of the decreasing viscosity, which reduces the ability for atoms to be added to a nucleus. Once a crystal nucleus does reach critical volume, crystallization progresses rapidly [67].

2.5 Glass Structure

While the mathematical formalism for describing the atomic structure will only be introduced in the following chapter, I will first briefly mention the common structural motifs of glasses.

Although glasses are amorphous they are found to have a significant degree of short range order and even intermediate range order [60] (greater than nearest neighbour ordering). This structure was initially described by Zachariasen [75] through the use of a continuous random network (CRN), as shown in Fig. 2.5a. Zachariasen [75] suggested that the simplest glasses, such as the archetypal glass SiO_2, were due to relatively small modifications of the corresponding crystal structure, maintaining the basic polyhedra but requiring a wide distribution of inter-polyhedral bond angles; this restriction on the polyhedra leads to the intermediate range order described by the CRN. Expanding on this description, [24] suggested an adaptation to allow for the inclusion of network modifying cations, such as alkalis or alkaline earths (as opposed to Si which is a network former). This modified random network (Fig. 2.5b) posits the possibility of modifier channels throughout the glass network, which have been suggested by EXAFS studies [24]. These modifier channels are surrounded by non-bridging oxygen atoms, which are oxygen atoms that are not bonded to two network former atoms.

The description of oxygen atoms as bridging (BO) or non-bridging (NBO) is an important concept in the oxide glasses, as it allows some insight into the depolymerization of the glass forming network. This in turn relates to the glass transition temperature and the fragility [4]. In the archetypal case of silicate glasses, Q^n is commonly used [25] to represent n BO atoms around each Si atom, with $0 \leq n \leq 4$ due to the tetrahedral coordination of Si. While the determination of the Q-species distribution is not directly obtainable from diffraction measurements (although it is from RMC from diffraction data), it is achievable through nuclear magnetic resonance (NMR) studies. Due to this capability and the ability for coordination number distribution determination in a number of cases [17], NMR is often used in conjunction with diffraction measurements [13].

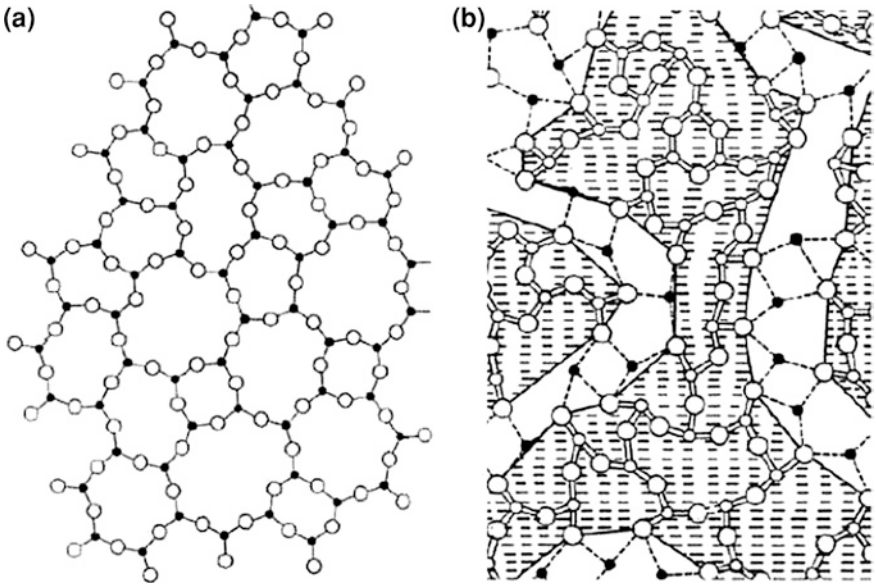

Fig. 2.5 **a** The continuous random network as described by Zachariasen (Reprinted with permission from [75], ©1932 American Chemical Society.) where silicon atoms (*closed circles*) are connected by bridging oxygen atoms (*open circles*). **b** The modified random network of Greaves (Reprinted from [24], © 1985, with permission from Elsevier.) where modifier channels occur due to the addition of alkalis or alkaline earths (*closed circles*) to the Si (*small open circles*) and O (*large open circles*) network

Although it is possible to have a range of different polyhedra [25], the most commonly occurring is the tetrahedra (Fig. 2.6). Tetrahedra are the main structural unit of a number of glasses, including many oxide, chalcogenide, and halide glasses. They can connect in three different ways (Fig. 2.6): corner sharing such as SiO_2 [25]; edge sharing such as $SiSe_2$ [44]; and face sharing such as Ge-Se-AgI [9]; or in combinations of these such as $GeSe_2$ [44].

2.6 Polyamorphism and First Order Liquid–Liquid Phase Transitions

When discussing liquid–liquid phase transitions it is important to establish how exactly they are being defined. In this particular case I am defining a liquid–liquid transition as being iso-compositional and first order in nature (i.e. there is a discontinuous change in the first derivatives of the free energy, such as the specific heat capacity at constant pressure or the density). As the two phases must have the same Gibbs free energy at the phase transition they must be able to coexist. This means that we arrive at the picture of a liquid phase of one density nucleating inside a liquid phase with a different density, as opposed to the usual idea

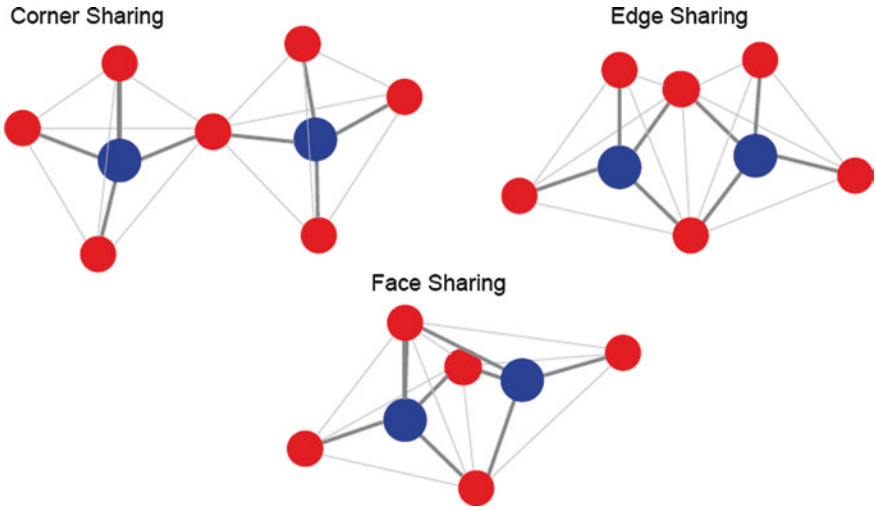

Fig. 2.6 The common structural motif in glasses, the tetrahedra, shown with the three different connecting configurations

of a continuous change in the density as one of the thermodynamic variables are altered. Given the situation of one liquid nucleating within another, glassy polyamorphism occurs if the sample is then quenched at such a rate that not only do both phases preferentially form a glass instead of a crystal, but also that this occurs before the phase transition causes a complete change from one liquid phase to the other. This would therefore manifest itself as small inclusions of one amorphous phase inside a matrix of the second amorphous phase.

The concept of a first order liquid–liquid phase transition is based upon the explanation of melting curve maxima of [58, 59] in 1967. Such melting curve maxima (Fig. 2.7) have been observed in a wide variety of different types of liquids, including Cs [38], P [35], Te [39], Ba, $NaClO_3$ [59], and H_2O [50], showing that it is a behaviour not related to a specific type of bonding.

The theory goes as follows: in the stable liquid state there are two distinct structural species of the liquid, a high density liquid (HDL) and a low density liquid (LDL). Due to fluctuations each component will vary between the two species, with only the time averaged distribution of species staying constant for a specific temperature and pressure. Upon an increase in pressure the proportion of the more dense species increases, which leads to an increase in the density of the liquid above that of the corresponding crystal. This causes the melting curve to have a negative relationship with pressure, as can be seen from the Clausius-Clapeyron relationship:

$$\frac{dT_m}{dP} = \frac{\Delta V_m}{\Delta S_m} \tag{2.6}$$

where T_m is the melting temperature, P is the pressure, ΔV_m is the change in volume upon melting, and ΔS_m is the change in entropy. As the change in entropy is always positive upon melting, an increase in the density upon melting means dT_m

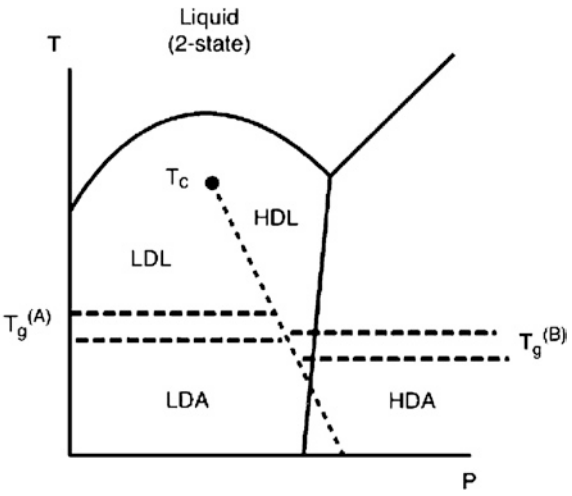

Fig. 2.7 A temperature-pressure diagram of a liquid with a melting curve maximum (Reproduced in part from McMillan [46] with permission of The Royal Society of Chemistry). The LDL vitrifies in the region denoted by $T_g^{(A)}$ to a low density amorphous phase (*LDA*), whereas the HDL vitrifies in a separate region, $T_g^{(B)}$, to a distinct high density amorphous phase (*HDA*)

$/\, dP < 0$. In instances such as the phase diagram of water, where the melting curve does not display an initial maximum, it is predicted that this occurs in the metastable tensile-strained regime where the equilibrium state is the vapour.

Adapting Guggenheim's theory of binary solutions [27], Rapoport [58] determined that there is a critical value leading to a separation into two liquids when:

$$\frac{w}{k_B T} > 2 \tag{2.7}$$

where w is the energy cost for replacing one species with another, and k_B is Boltzmann's constant. This led to the suggestion of a first order transition between a higher density liquid and a lower density liquid, whilst maintaining the same composition. The enthalpy change that occurs in a liquid–liquid transition is expected to be lower than that during a solid-liquid transition, as the degree of atomic rearrangement is expected to be lower changing between two disordered structures than in nucleating an ordered crystal. From this and the inequality above (2.7) it is probable that, at a specific pressure, the liquid–liquid transition temperature is below the melting temperature. This would mean that in general the liquid–liquid phase transition line would be expected to occur in the supercooled regime, ending with a critical point below T_m.

Firstly I will highlight in detail the particular cases of liquid–liquid phase transitions in water and yttria aluminates, before briefly mentioning a few other examples.

2.6.1 Water

Until this point I have only discussed glass formation from the perspective of quenching a liquid, and while this is both the oldest and most commonly used method, we must also consider pressure induced amorphisation (PIA). PIA for

was initially reported by Mishima et al. [50] by cooling crystalline ice Ih to 77 K before pressurising to ~1 GPa. This produced a significant, apparently discontinuous, change in volume over a small pressure range, which was then shown to be amorphous using X-ray diffraction. It is important to note that [50] suggested the X-ray diffraction data showed the new amorphous phase was not the structure that results from rapidly cooling liquid water [45], and that the crystal to amorphous transition was not reversible.

Expanding on this discovery the same authors [51] investigated the effects of heating this new amorphous ice (which will now be termed high density amorphous or HDA). They apparently determined that heating HDA to ~117 K at atmospheric pressure caused a sharp transition to a low density amorphous structure (~22 % lower density), although they only suggest that it "strongly resembles a first-order transition".

While there are three main theoretical explanations [14] for the anomalous behaviour of H_2O, I will only be focusing on the possibility of a liquid–liquid phase transition ending in a critical point. This was initially suggested by Poole et al. [57] based on both the experimental studies discussed above [51], and their own MD simulations. These simulations used the ST2 [63] potential for water, although similar effects have been seen using the TIP4P [34] potential. As pointed out by Mishima and Stanley [47], and Franzese et al. [20], the occurrence of a first order liquid–liquid phase transition is a natural consequence of a double welled potential (Fig. 2.8a), such as ST2. They also highlight the fact that, due to the complexity of the real interaction potentials, water is notoriously difficult to simulate accurately [47]. This is evident when considering that some simulations with the ST2 potential have predicted three liquid–liquid critical points [10].

The position in *PT* space of the proposed [57] liquid–liquid transition is below the homogenous nucleation temperature for supercooled water (Fig. 2.8b). This means that it is very difficult to experimentally investigate the region of the possible liquid–liquid phase transition. Due to this, Mishima and Stanley [48] adopted a method utilising the melting curve of metastable ice IV, which happens to pass through the anticipated liquid–liquid phase transition line. At the predicted crossover they detected a change in the melting behaviour indicating that the ice IV was melting to a different liquid, before crystallizing to the stable crystalline ice phase. Despite this hint of a possible liquid–liquid transition, the results could be influenced by a few different factors; the experimental setup used very small quantities (droplets of ~1 μm diameter) of water as an emulsion rather than pure H_2O, which raises questions about the effects of both the confinement and the surface interactions; the measured crossover is very close to the homogenous nucleation temperature, which may result in a similar effect; and the separation of data points raises the possibility of whether there is a sharp, but not continuous transition [14].

There is a significant degree of contention as to whether the transition between LDA and HDA is discontinuous [14, 28, 29, 66]. Although initial studies [51, 52] of the compression with applied pressure suggest the transition was sharp, as does a Raman study by Mishima and Suzuki [49], there have been a significant number of X-ray [29] and neutron diffraction studies [66], and MD simulations [28] that have implied that the structural changes actually occur continuously between

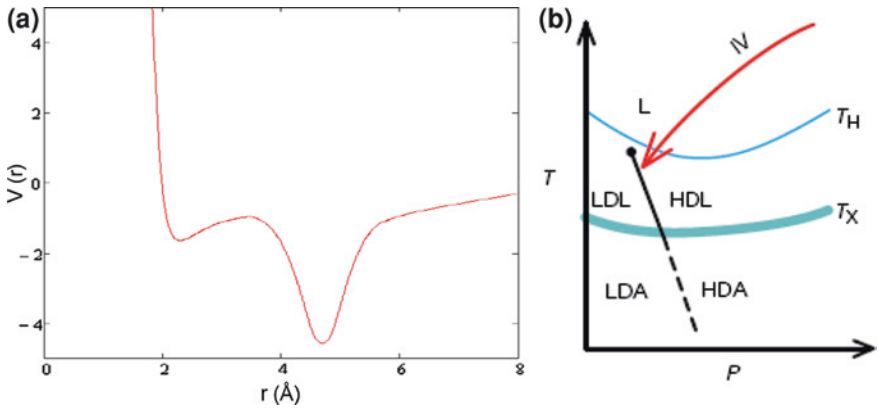

Fig. 2.8 **a** A schematic of a double welled potential. At high temperatures both wells can be sampled. As the temperature reduces the deeper, low density well becomes the preferentially filled, resulting in a LDL. As the pressure is increased the system becomes situated in the less deep well, corresponding to a higher density liquid. **b** The proposed position in *TP* space of the liquid–liquid phase transition in water, reproduced from Mishima and Stanley (Reprinted by permission from Macmillan Publishers Ltd: [48], © 1998). T_H is the homogenous nucleation temperature line for supercooled water, while T_X is the temperature at which amorphous ice spontaneously crystallizes upon heating

an infinite number of intermediary states. A recent MD study by Limmer and Chandler [41] questions the appearance of a liquid–liquid transition in MD simulations of one component liquids, by suggesting that what is being observed is in fact a liquid-solid transition.

The possibility of the existence of a second liquid–liquid phase transition in water was discussed following the discovery [42] of an even higher density amorphous state, named very high density amorphous (VHDA). However, unlike the LDA-HDA transition, this has since been widely accepted to be a continuous change in the structure [74].

When considering the range of conflicting results and the experimental challenges, it is easy to understand why the existence of a first order liquid–liquid phase transition in water has not been conclusively established.

2.6.2 Al_2O_3-Y_2O_3 System

The initial reports of a liquid–liquid phase transition in the Al_2O_3-Y_2O_3 system were due to Aasland and Mcmillan's [1] (AM) observation of polyamorphism in a concentration range of 24–32 mol% Y_2O_3. They produced samples using a combination of sol-gel synthesis followed by Ir wire heating. The volume fraction of the reported glassy inclusions increased with both decreasing Y_2O_3 content and quench rate; it is important to note that crystallization occurred in samples of 20

and 22 mol% Y_2O_3. In order to determine the amorphous nature of the inclusions AM (1994) used micro-infrared and Raman spectroscopy. However, as pointed out by Nagashio and Kuribayashi [55] (NK), due to the transparency of the samples it is difficult to ensure that spectra are taken from inclusions located on the surface, rather than some thickness of bulk glass separating an inclusion from the surface. Using aero-acoustic levitation, NK (2002) produced AY samples across the same composition which showed the same morphology of an inclusion containing matrix as AM (1994). Using microfocus XRD they demonstrated that the inclusions present on the surface of their sample had sharp peaks consistent with crystalline YAG.

Further evidence to suggest that the observation of amorphous inclusions in the Al_2O_3-Y_2O_3 system is in fact that onset of crystallization, comes from the microfocus EXAFS of Barnes et al. [6]. Although similar in principal to both the micro-infrared and Raman spectroscopy of AM (1994) and the microfocus XRD of NK (2002), this method had the significant advantage that inclusions on the surface showed strong optical fluorescence, definitively establishing that the spectrum came from an inclusion. Further characterisation of these inclusions using cross-polarised microscopy also determined that they were crystalline of nature [61].

Along with the possible glass polyamorphism in Al_2O_3-Y_2O_3 previously discussed, Greaves et al. [26] observed an apparent liquid–liquid phase transition in situ using aerodynamic levitation combined with small and wide angle X-ray scattering (SAXS/WAXS). In addition to this they also suggested that a repeating 0.25 Hz oscillation in the pyrometry was due to a ‘polyamorphic rotor’. These observations will be discussed further in Chap. 5, when compared with in situ SANS experiments and pyrometric studies.

Similarly to water, MD simulations [71] have also suggested the possibility of a liquid–liquid phase transition in the yttria-aluminates.

2.6.3 Other Examples

There are a number of other systems which are possible candidates for demonstrating liquid–liquid phase transitions.

Triphenyl phosphate (TPP) is an organic compound of $P(OC_6H_5)_3$ which Cohen et al. [11, 30] first suggested exhibited polyamorphism in 1996. TTP liquid can be supercooled, although if it is quenched slowly it crystallizes at ~245 K. However if it is fast quenched below ~225 K it is stable against crystallization for extended periods of time. If it is kept in this supercooled state between 213 and 225 K for a matter of hours (during which it becomes turbid, opaque, and then finally clear again) it appears to form a ‘glacial phase’ [11] of apparently different density, although the X-ray diffraction is very similar [30]. The ‘glacial phase’ is so called because it is apparently glassy [11] but is distinct from the TPP glass formed by fast quenching below 176 K. As with both water and the yttria-aluminate system there are a number of different views [31, 33, 65] on what phenomenon is manifesting itself. A number of these come under the general theme of an apparently disordered phase that contains nanocrystallites [16].

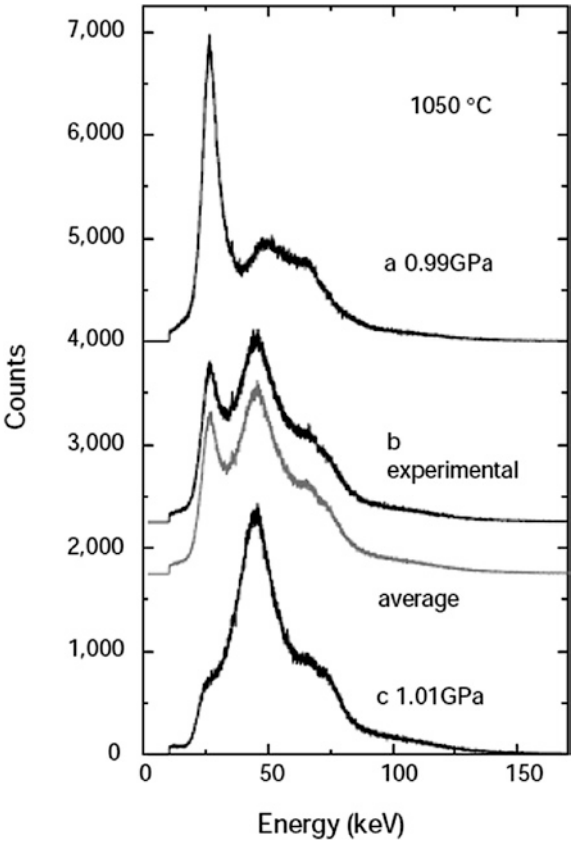

Fig. 2.9 The X-ray data of Katayama et al. (Reprinted by permission from Macmillan Publishers Ltd: [35], © 2000) which initially suggested a first order liquid–liquid phase transition in phosphorus. The *grey line* represents a weighted average of the two distinct species observed at high and low pressure, and accurately recreates the experimental data taken between these two pressures. This strongly suggested coexistence which is an essential requirement for a first order transition

In 2000 Katayama et al. [35] conducted an in situ X-ray diffraction experiment on liquid phosphorus which strongly suggested a first order liquid–liquid phase transition between a molecular liquid and a polymeric liquid. This was particularly notable because not only did it occur in the stable liquid, as opposed to the more common metastable supercooled liquid, it also demonstrated coexistence of the two phases. This was clearly visible from a weighted sum of the diffraction patterns from either side of the transition compared to the diffraction pattern at the transition (Fig. 2.9). The coexistence was also apparent from in situ X-ray radiography [36] and had been suggested by ab initio MD simulations [54]. However a further, more extensive, in situ X-ray diffraction investigation by Monaco et al. [53] established that the transition was in fact between a polymeric liquid and a molecular fluid; the latter being the fluid form associated with the metastable white phosphorus crystal, which takes a molecular tetrahedral structure. Therefore while undoubtedly a first order liquid-fluid phase transition, phosphorus did not provide the first evidence for a first order liquid–liquid phase transition.

It has also been suggested [25] that polyamorphism could occur, or has been already detected, in some network glasses, such as SiO_2-GeO_2 [43]. However, again

due to experimental challenges [72] relating to the proposed location in the phase diagram of the polyamorphism, it has been difficult to conclusively establish.

To summarise, there has been significant amount of research into the possibility of a first order isocompositional liquid–liquid phase transition. So far there has been no overwhelming evidence in support of this hypothetical explanation of negative melting curves in any system. The results of [26] strongly suggest the existence of a liquid–liquid phase transition in the yttria aluminates; it is therefore essential that this discovery is independently established, as will be discussed in Chap. 5.

References

1. Aasland S, McMillan PF (1994) Density-driven liquid–liquid phase separation in the system Al_2O_3-Y_2O_3. Nature 369:633–636
2. Adam G, Gibbs JH (1965) On the temperature dependence of cooperative relaxation properties in glass-forming liquids. J Chem Phys 43(1):139–146
3. Angell CA (1991) Relaxation in liquids, polymers and plastic crystals—strong/fragile patterns and problems. J Non-Cryst Solids 131–133:13–31
4. Angell CA (1995) Formation of glasses from liquids and biopolymers. Science 267(5206):1924–1935
5. Angell CA, Ngai KL, Mckenna GB, McMillan PF, Martin SW (2000) Relaxation in glass forming liquids and amorphous solids. J Appl Phys 88(6):3113–3157
6. Barnes AC, Skinner LB, Salmon PS, Bytchkov A, Pozdnyakova I, Farmer TO, Fischer HE (2009) Liquid–liquid phase transition in supercooled yttria-alumina. Phys Rev Lett 103(22):225702
7. Bengtzelius U, Götze W, Sjölander A (1984) Dynamics of supercooled liquids and the glass transition. J Phys C: Solid State Phys 17(33):5915–5934
8. Birge NO, Nagel SR (1985) Specific-heat spectroscopy of the glass transition. Phys Rev Lett 54(25):2674–2677
9. Boev V, Mitkova M, Lefterova E, Wagner T, Kasap S, Vlček M (2000) Glass formation in the Ge ± Se ± AgI ternary. J Non-Cryst Solids 266:867–871
10. Brovchenko I, Geiger A, Oleinikova A (2003) Multiple liquid–liquid transitions in supercooled water. J Chem Phys 118(21):9473–9476
11. Cohen I, Ha A, Zhao X, Lee M, Fischer T, Strouse MJ, Kivelson D (1996) A Low-temperature amorphous phase in a fragile glass-forming substance. J Phys Chem 100(20):8518–8526
12. Cohen MH, Turnbull D (1959) Molecular transport in liquids and glasses. J Chem Phys 31(5):1164–1169
13. Cole JM, van Eck ERH, Mountjoy G, Newport RJ, Brennan T, Saunders GA (1999) A neutron diffraction and ^{27}Al MQMAS NMR study of rare-earth phosphate glasses, $(R_2O_3)_x(P_2O_5)_{1-x}$, $x = 0.187$-0.263, R = Ce, Nd, Tb containing Al impurities. J Phys Condens Matter 11(47):9165–9178
14. Debenedetti PG (2003) Supercooled and glassy water. J Phys Condens Matter 15(45):R1669–R1726
15. Debenedetti PG, Stillinger FH (2001) Supercooled liquids and the glass transition. Nature 410(6825):259–267
16. Demirjian BG, Dosseh G, Chauty A, Ferrer M-L, Morineau D, Lawrence C, Takeda K, Kivelson D, Brown S (2001) Metastable solid phase at the crystalline-amorphous border: the glacial phase of triphenyl phosphite. J Phys Chem B 105(11):2107–2116
17. Eckert H (1992) Structural characterization of noncrystalline solids and glasses using solid state NMR. Prog Nucl Magn Reson Spectrosc 24(3):159–293

18. Ediger MD, Angell CA, Nagel SR (1996) Supercooled liquids and glasses. J Phys Chem 100(31):13200–13212
19. Finn CBP (1993) Thermal physics, 2nd edn. Chapman and Hall, London
20. Franzese G, Malescio G, Skibinsky A, Buldyrev SV, Stanley HE (2001) Generic mechanism for generating a liquid–liquid phase transition. Nature 409(6821):692–695
21. Fulcher GS (1925) Analysis of recent measurements of the viscosity of glasses. J Am Ceram Soc 8:339
22. Goldstein M (2011) The past, present, and future of the Johari-Goldstein relaxation. J Non-Cryst Solids 357(2):249–250
23. Götze W, Sjögren L (1992) Relaxation processes in supercooled liquids. Rep Prog Phys 55(3):241–376
24. Greaves GN (1985) EXAFS and the structure of glass. J Non-Cryst Solids 71:203–217
25. Greaves GN, Sen S (2007) Inorganic glasses, glass-forming liquids and amorphizing solids. Adv Phys 56(1):1–166
26. Greaves GN, Wilding MC, Fearn S, Langstaff D, Kargl F, Cox S, Van QVu, Majérus O, Benmore CJ, Weber R, Martin CM, Hennet L (2008) Detection of first-order liquid/liquid phase transitions in yttrium oxide-aluminum oxide melts. Science 322:566–570
27. Guggenheim EA (1935) The Statistical Mechanics of Regular Solutions. Proc R Soc A Math Phys Eng Sci 148(864):304–312
28. Guillot B, Guissani Y (2003) Polyamorphism in low temperature water: a simulation study. J Chem Phys 119(22):11740
29. Guthrie M, Urquidi J, Tulk C, Benmore C, Klug D, Neuefeind J (2003) Direct structural measurements of relaxation processes during transformations in amorphous ice. Phys Rev B 68(18):1–5
30. Ha A, Cohen I, Zhao X, Lee M, Kivelson D (1996) Supercooled liquids and polyamorphism. J Phys Chem 100(1):1–4
31. Hédoux A, Guinet Y, Descamps M, Hernandez O, Derollez P, Dianoux AJ, Foulon M, Lefèbvre J (2002) A description of the frustration responsible for a polyamorphism situation in triphenyl phosphite. J Non-Cryst Solids 307:637–643
32. Hodge IM (1994) Enthalpy relaxation and recovery in amorphous materials. J Non-Cryst Solids 169(3):211–266
33. Johari GP, Ferrari C (1997) Calorimetric and dielectric investigations of the phase transformations and glass transition of triphenyl phosphite. J Phys Chem 5647(49):10191–10197
34. Jorgensen WL, Chandrasekhar J, Madura JD, Impey RW, Klein ML (1983) Comparison of simple potential functions for simulating liquid water. J Chem Phys 79(2):926
35. Katayama Y, Mizutani T, Utsumi W, Shimomura O, Yamakata M, Funakoshi K (2000) A first-order liquid–liquid phase transition in phosphorus. Nature 403(6766):170–173
36. Katayama Y, Inamura Y, Mitzutani T, Yamakata M, Utsumi W, Shimomura O (2004) Macroscopic separation of dense fluid phase and liquid phase of phosphorus. Science 306(5697):848–851
37. Kauzmann W (1948) The nature of the glassy state and the behavior of liquids at low temperatures. Chem Rev 43(2):219–256
38. Kennedy GC, Jayaraman A, Newton RC (1959) Fusion curve and polymorphic transitions of cesium at high pressures. Phys Rev 126(4):1363–1366
39. Klement W Jr, Cohen LH, Kennedy GC (1966) Melting and freezing of selenium and tellurium at high pressures. J Phys Chem Solids 27(1):171–177
40. Leutheusser E (1984) Dynamical model of the liquid-glass transition. Phys Rev A 29(5):2765
41. Limmer DT, Chandler D (2011) The putative liquid–liquid transition is a liquid-solid transition in atomistic models of water. J Chem Phys 135(13):134503
42. Loerting T, Salzmann C, Kohl I, Mayer E, Hallbrucker A (2001) A second distinct structural "state" of high-density amorphous ice at 77 K and 1 bar. Phys Chem Chem Phys 3(24):5355–5357
43. Majérus O, Cormier L, Itié J-P, Galoisy L, Neuville DR, Calas G (2004) Pressure-induced Ge coordination change and polyamorphism in SiO_2–GeO_2 glasses. J Non-Cryst Solids 345–346:34–38
44. March NH, Tosi MP (2002) Introduction to liquid state physics. World Scientific, Singapore

45. Mayer E, Brüggeller P (1982) Vitrification of pure liquid water by high pressure jet freezing. Nature 298(5876):715–718
46. McMillan PF (2004) Polyamorphic transformations in liquids and glasses. J Mater Chem 14(10):1506–1512
47. Mishima O, Stanley HE (1998) The relationship between liquid, supercooled and glassy water. Nature 396(6907):329–335
48. Mishima O, Stanley HE (1998) Decompression-induced melting of ice IV and the liquid–liquid transition in water. Nature 392(6672):164–168
49. Mishima O, Suzuki Y (2002) Propagation of the polyamorphic transition of ice and the liquid–liquid critical point. Nature 419(6907):599–603
50. Mishima O, Calvert LD, Whalley E (1984) "Melting ice" I at 77 K and 10 kbar: a new method of making amorphous solids. Nature 310:393–395
51. Mishima O, Calvert LD, Whalley E (1985) An apparently first-order transition between two amorphous phases of ice induced by pressure. Nature 314(6006):76
52. Mishima O, Takemura K, Aoki K (1991) Visual observations of the amorphous–amorphous transition in H_2O under pressure. Science 254(5030):406–408
53. Monaco G, Falconi G, Crichton W, Mezouar M (2003) Nature of the first-order phase transition in fluid phosphorus at high temperature and pressure. Phys Rev Lett 90(25):255701
54. Morishita T (2001) Liquid–liquid phase transitions of phosphorus via constant-pressure first-principles molecular dynamics simulations. Phys Rev Lett 87(10):105701
55. Nagashio K, Kuribayashi K (2002) Spherical yttrium aluminum garnet embedded in a glass matrix. J Am Ceram Soc 85(9):2353–2358
56. Paluch M, Roland C, Pawlus S, Zioło J, Ngai K (2003) Does the Arrhenius temperature dependence of the Johari-Goldstein relaxation persist above T_g? Phys Rev Lett 91(11):115701
57. Poole PH, Sciortino F, Essmann U, Stanley HE (1992) Phase behaviour of metastable water. Nature 360(6402):324–328
58. Rapoport E (1967) Model for melting-curve maxima at high pressure. J Chem Phys 46(8):2891–2895
59. Rapoport E (1967) Melting curve of $NaClO_3$. J Chem Phys 46(9):3279–3281
60. Salmon PS (2007) The structure of tetrahedral network glass forming systems at intermediate and extended length scales. J Phys: Condens Matter 19(45):455208
61. Skinner LB, Barnes AC, Salmon PS, Crichton WA (2008) Phase separation, crystallization and polyamorphism in the Y_2O_3-Al_2O_3 system. J Phys: Condens Matter 20:205103
62. Stillinger FH (1995) A topographic view of supercooled liquids and glass formation. Science 267(5206):1935–1939
63. Stillinger FH, Rahman A (1974) Improved simulation of liquid water by molecular dynamics. J Chem Phys 60(4):1545–1557
64. Tammann G, Hesse W (1926) Die abhängigkeit der viskosität von der temperatur bei unterkühlten flüssigkeiten. Z Anorg Allg Chem 156:245–257
65. Tanaka H, Kurita R, Mataki H (2004) Liquid–liquid transition in the molecular liquid triphenyl phosphite. Phys Rev Lett 92(2):025701
66. Tse J, Klug D, Guthrie M, Tulk C, Benmore C, Urquidi J (2005) Investigation of the intermediate- and high-density forms of amorphous ice by molecular dynamics calculations and diffraction experiments. Phys Rev B 71(21):214107
67. Turnbull D (1969) Under what conditions can a glass be formed? Contemp Phys 10(5):473–488
68. Turnbull D, Cohen MH (1961) Free-volume model of the amorphous phase: glass transition. J Chem Phys 34(1):120–125
69. Turnbull D, Fisher JC (1949) Rate of nucleation in condensed systems. J Chem Phys 17(1):71–73
70. Vogel H (1921) Das temperatur-abhängigkeitsgesetz der viskosität von flüssigkeiten. Phys Zeit 22:645–646
71. Wilding MC, Wilson M, McMillan PF (2005) X-ray and neutron diffraction studies and MD simulation of atomic configurations in polyamorphic Y_2O_3-Al_2O_3 systems. Philosophical transactions. Series A, Mathematical, physical, and engineering sciences 363(1827):589–607

72. Wilding M, Guthrie M, Bull CL, Tucker MG, McMillan PF (2008) Feasibility of in situ neutron diffraction studies of non-crystalline silicates up to pressures of 25 GPa. J Phys Condens Matter 20(24):244122
73. Williams G, Watts C (1970) Non-symmetrical dielectric relaxation behaviour arising from a simple empirical decay function. Trans Faraday Soc 66(565P):80–85
74. Winkel K, Elsaesser M, Mayer E, Loerting T (2008) Water polyamorphism: reversibility and (dis)continuity. J Chem Phys 128(4):044510
75. Zachariasen WH (1932) The atomic arrangement in glass. J Am Chem Soc 54:3841–3851

http://www.springer.com/978-3-319-06574-8

Structural Studies of Liquids and Glasses Using Aerodynamic Levitation

Farmer, Th.

2015, XIV, 113 p. 54 illus., 30 illus. in color., Hardcover
ISBN: 978-3-319-06574-8